

On the Impact of Pinching Antennas on Traffic Offloading

Zhiguo Ding, *Fellow, IEEE*, Robert Schober, *Fellow, IEEE*, and H. Vincent Poor, *Life Fellow, IEEE*

Abstract—Pinching antennas are characterized by their capability to create strong line-of-sight connections and realize multi-antenna systems in a flexible manner. Existing works have demonstrated the significant potential of pinching antennas for physical layer design. The aim of this paper is to investigate how pinching antennas can be used to reshape the architecture of future networks. In particular, this paper is motivated by the key advantage of pinching antennas, which is to reconfigure the physical boundaries of wireless cells, and focuses on the impact of pinching antennas on traffic offloading. The models for traffic offloading and pinching antenna transmission are presented first. Then, two traffic offloading strategies are developed based on whether an offloading user releases its bandwidth in its original cell. An overall transmit power minimization problem is formulated, where the optimal solutions for the transmit powers and antenna locations are obtained. The presented simulation results demonstrate that the use of pinching antennas can efficiently support traffic offloading, yield low energy consumption, and achieve balanced cell resource utilization.

Index Terms—Pinching antennas, multi-cell interference management, resource allocation.

I. INTRODUCTION

The ever-growing demand for higher system throughput and enhanced transmission reliability motivates the use of flexible antennas, which are distinguished by their capability to reconfigure the wireless channel conditions [1]–[5]. Among the potential candidates for flexible antennas, pinching antennas have received significant attention since they can be flexibly placed close to users to establish strong line-of-sight connections between transceivers [6], [7]. The generalization of pinching antennas beyond DOCOMO’s original design has recently been proposed in [8], where the adoption of guided-wave media other than dielectric waveguides, such as leaky coaxial cables and metallic pipes, is introduced to support diverse indoor and outdoor applications using both the sub-6 GHz and millimeter-wave bands. Novel designs to improve the efficiency of signal emission and the degrees of freedom of pinching-antenna-enabled transmission have been proposed in [9] and [10]. Furthermore, the benefits of pinching antennas for other key sixth-generation (6G) enabling techniques, such as physical layer security [11]–[13], integrated sensing and communications (ISAC) [14]–[17], federated learning [18]–[20], etc., have also been recently investigated.

Compared to the extensive study of the impact of pinching antennas on physical layer design, research on their impact on the network architecture started only recently. For example, stochastic-geometry studies of multi-cell pinching-antenna systems have been carried out in [21] and [22], and an algorithmic framework was developed in [23] to utilize pinching

antennas for realizing low-complexity and low-transmit-power multi-cell coordination. These existing studies revealed that pinching antennas have great potential to flexibly change the shape of a cell, and hence reconfigure the network architecture, as exemplified in Fig. 1. In particular, consider a two-cell scenario, where the two base stations, denoted by BS_0 and BS_1 , are located at $(-r_c, 0)$ and $(r_c, 0)$, respectively, where r_c denotes the radius of the cells. Assume that BS_0 is equipped with a pinching antenna whose location range is between $(-r_c, 0)$ and $(0, 0)$, and BS_1 is equipped with a conventional antenna located at $(r_c, 0)$. We focus on the users located within the colored semi-circle area in Fig. 1(a). With conventional antennas, the users in the semi-circle area are always served by BS_2 , where Fig. 1(b) shows the transmit power (in dBm) required to achieve the target data rate of 1 bit/s/Hz in the conventional-antenna case. Fig. 1(c) focuses on the pinching-antenna case, where each user in the colored area can be served by either BS_1 or BS_2 , whichever yields the lower transmit power. Fig. 1 shows that if equipped with a pinching-antenna system, BS_0 can effectively extend its service region, i.e., it can penetrate the coverage region of BS_1 , such that BS_1 ’s users can be offloaded and served by BS_0 with less power consumption.

The significant potential performance gain indicated by Fig. 1 motivates us to thoroughly study the impact of pinching antennas on traffic offloading. Recall that traffic offloading is crucial to balance network loads and enhance user experience, particularly in cellular scenarios where some cells are congested while others remain underutilized [24]. Supporting traffic offloading becomes even more important for forthcoming 6G applications, which are expected to rely on ultra-dense cell deployments, artificial-intelligence (AI) native control, and extremely high data rates [25]. The aim of this paper is to demonstrate that the capability of pinching antennas to reconfigure cell boundaries can be used to efficiently support traffic offloading, achieve low energy consumption, and realize balanced cell resource utilization.

A general traffic offloading model is first developed in the paper, where M overloaded cells try to offload their users to a neighboring underutilized cell with free capacity. Potential applications of the presented traffic offloading model, such as macro-cell-to-small-cell and small-cell-to-small-cell traffic offloading, are illustrated. Then, a system model for pinching-antenna-assisted traffic offloading is established, where the use of a pinching-antenna system with a segmented waveguide is proposed in order to increase the degrees of freedom and reduce maintenance costs. Whether a user is willing to release its bandwidth in its original cell affects the traffic offloading strategy as follows:

- We first consider a simple strategy, where a user does not release its allocated bandwidth in its original cell,

Z. Ding is with Nanyang Technological University, Singapore. R. Schober is with the Institute for Digital Communications, Friedrich-Alexander-University Erlangen-Nurnberg (FAU), Germany. H. V. Poor is with the Department of Electrical and Computer Engineering, Princeton University, Princeton, NJ 08544, USA.

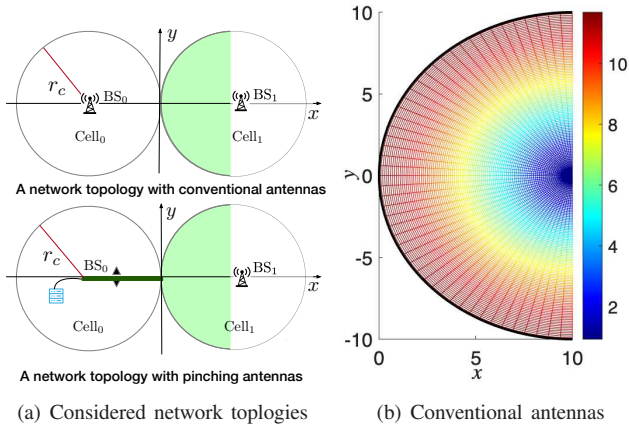


Fig. 1. Illustration of the impact of pinching antennas on cell boundaries. The two base stations, denoted by BS_0 and BS_1 , are located at $(-r_c, 0)$ and $(r_c, 0)$, respectively, where r_c denotes the radius of the cells, $r_c = 10$ m, and the target data rate is 1 bit/Hz/s. BS_0 is equipped with a pinching antenna whose location range is between $(-r_c, 0)$ and $(0, 0)$, BS_1 is equipped with a conventional antenna, and the antennas are placed at a height of 3 meters. We focus on users located within the given semi-circle. Each user can be served by either BS_0 or BS_1 , whichever yields the lower transmit power (measured in dBm).

i.e., each offloaded user is served in the new cell by using its own bandwidth. The advantage of this strategy is that the M offloaded users can be served by their new base station in an interference-free manner. However, while this traffic offloading strategy can reduce the overall transmit power of the system, offloading a user from its original cell to the new cell cannot increase the bandwidth available in the original cell. An overall transmit power minimization problem is formulated by optimizing the transmit powers of the base stations and the location of the pinching antenna. Closed-form expressions for the optimal transmit powers are obtained for a given antenna location, and then used to reformulate the considered optimization problem to a convex form, where the optimal antenna location can be obtained efficiently. Furthermore, a special case with two cells is investigated, where a closed-form expression for the optimal location of the pinching antenna is obtained. The analytical result shows that the optimal location of the pinching antenna is the average of the projections of the users' positions onto the waveguide, where the distances between the users and the waveguide have no impact.

- We then consider a more sophisticated traffic offloading strategy, where completely-offloaded users release

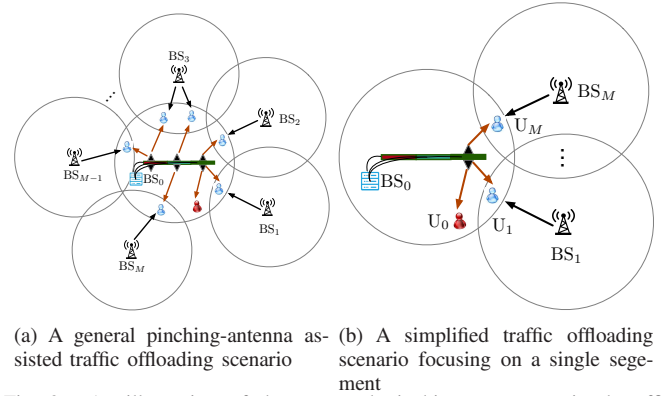


Fig. 2. An illustration of the proposed pinching-antenna assisted traffic offloading scheme.

their allocated bandwidth in their original cell. The key advantage of this strategy is that the departure of a user frees up resources, which allows the user's original cell to accommodate additional users and hence improve the overall resource utilization. However, this offloading strategy is more complex since each offloaded user needs to be served in its new cell by sharing the bandwidth with other users. Non-orthogonal multiple access (NOMA) is employed to facilitate efficient bandwidth sharing while effectively suppressing co-channel interference [26]. A challenge when applying NOMA is that there are multiple possible successive interference cancellation (SIC) decoding orders. For each of the possible SIC decoding orders, an overall transmit power minimization problem is formulated with the transmit powers and the antenna location as optimization variables. Closed-form expressions for the transmit powers are obtained first and then used to recast the original optimization problem into convex form, which ensures that the optimal solution can be obtained efficiently. For the special case of two cells, concise closed-form expressions for the optimal antenna location and the overall transmit power can be obtained. Unlike the previously considered offloading strategy, the obtained analytical results show that the distances between the users and the waveguide are crucial for determining the optimal SIC decoding order and the optimal location of the pinching antenna.

II. SYSTEM MODEL

A. Traffic Offloading Model

Consider a multi-cell downlink communication scenario with $M+1$ cells. The cells and their base stations are denoted by $Cell_m$ and BS_m , $0 \leq m \leq M$, respectively. We assume that $Cell_m$, $1 \leq m \leq M$, are overloaded and hence want to offload parts of their traffic to their neighbor, BS_0 , as shown in Fig. 2(a). Applications of the considered traffic offloading scenario are discussed in the following.

1) *Macro-Cell-to-Small-Cell Traffic Offloading*: In heterogeneous networks, each macro base station, e.g., BS_m , $1 \leq m \leq M$, covers a large geographic area, and hence is prone to traffic overloading. Macro-cell-to-small-cell traffic offloading ensures that heavy traffic in the macro-cell base stations is shifted to a small-cell base station, e.g., BS_0 [27], [28].

2) *Small-Cell-to-Small-Cell Traffic Offloading*: Future 6G systems will feature ultra-dense deployments of small cells,

where traffic demand can be unevenly distributed, e.g., some cells are heavily congested while others remain underutilized [25]. A cell with light traffic, e.g., Cell₀, can help its neighbors by serving the users that are originally associated with heavy-traffic cells, i.e., Cell_{*m*}, $1 \leq m \leq M$. As a result, users can be redistributed among cells to ensure load balancing and avoid overcrowding.

3) *Cell-to-Wi-Fi Traffic Offloading*: Future wireless systems are expected to exploit the coexistence of cellular systems and Wi-Fi networks [29]. Therefore, BS₀ can be a Wi-Fi access point with light traffic to help reduce the traffic of cellular base stations, BS_{*m*}, $1 \leq m \leq M$. In addition, Cell₀ could also be a cell in an airport/campus shop or building using unlicensed bands, to which traffic of overcrowded licensed bands can be offloaded.

B. Pinching-Antenna Assisted Traffic Offloading

For illustration purposes, we assume that BS_{*m*}, $1 \leq m \leq M$, is equipped with a single conventional fixed-location antenna, and BS₀ is equipped with a pinching-antenna system. In particular, denote the location of BS_{*m*}, $0 \leq m \leq M$, by ψ_m^{BS} .

In order to reduce maintenance cost, a segmented waveguide is employed by BS₀, where at most a single antenna is activated on each segment, as shown in Fig. 2(a). By assuming that cells connected to different segments are served on orthogonal bandwidth resources, e.g., orthogonal frequency-division multiple access (OFDMA) subcarriers, there is no interference among the cells. Furthermore, because each segment is connected to an independent feed point, resource allocation across different segments, such as transmit-power control and antenna placement, can be decoupled [10]. Therefore, this paper investigates the optimization of pinching-antenna assisted traffic offloading by focusing on the simplified traffic offloading scenario depicted in Fig. 2(b), where a single segment is to offload M users from the M cells adjacent to the segment. Denote the user in Cell_{*m*} by U_m , $1 \leq m \leq M$. Furthermore, assume that in Cell₀, there exists a user, denoted by U_0 , being currently served by the segment.

The dual connectivity (DC) mode is used, where each U_m is served by BS₀ and BS_{*m*} simultaneously [27], [28]. We note that complete offloading, i.e., U_m is served by BS₀ only, is a special case of the DC mode.

C. Benchmark: No Traffic Offloading

Without traffic offloading, U_m is served by BS_{*m*} only. We assume that OFDMA is adopted by the cells, where each user is allocated a unique OFDM subcarrier, and there is no interference among the $(M + 1)$ users. Therefore, U_m 's achievable data rate is given by

$$R_m^{\text{No-TO}} = \log_2 \left(1 + \frac{\eta P_m^{\text{No-TO}}}{P_N |\psi_m - \psi_m^{\text{BS}}|^2} \right), \quad (1)$$

where $P_m^{\text{No-TO}}$ denotes U_m 's transmit power, $\eta = \frac{c^2}{16\pi^2 f_c^2}$, c is the speed of light, f_c is the carrier frequency, P_N denotes the noise power, ψ_m denotes U_m 's location, and $|\psi_m - \psi_m^{\text{BS}}|$ denotes the distance between U_m and BS_{*m*}. By assuming that

TABLE I
THE TWO CONSIDERED TRAFFIC OFFLOADING STRATEGIES

	Strategy I			Strategy II		
	U ₀	U ₁	U ₂	U ₀	U ₁	U ₂
BS ₀	F ₀	F ₁	F ₂	F ₀	F ₀	F ₀
BS ₁		F ₁			F ₁	
BS ₂			F ₂			F ₂

all users have the same target data rate, denoted by R , the minimal transmit power for BS_{*m*} to serve U_m without traffic offloading is given by $P_m^{\text{No-TO}} = \epsilon |\psi_m - \psi_m^{\text{BS}}|^2$, where $\epsilon = \frac{P_N(2^R - 1)}{\eta}$.

Depending on how an offloaded user is served in the new cell, two different traffic offloading strategies can be designed, as discussed in the following sections.

III. BS₀ HAS ACCESS TO U_m 'S SUBCARRIER IN Cell_{*m*}

This section focuses on the offloading strategy, where BS₀ has access to U_m 's subcarrier during traffic offloading, i.e., Strategy I illustrated in Table I. In particular, for the illustrated three-cell special case, F_m denotes the subcarrier allocated to U_m in Cell_{*m*}. For Strategy I, during the offloading, U_m , $1 \leq m \leq M$, is simultaneously served by BS_{*m*} and BS₀ on F_m . This offloading strategy offers the benefit that the $(M + 1)$ users can be served in Cell₀ in an interference-free manner, but suffers from the disadvantage that the bandwidth available in Cell_{*m*} is not increased despite the departure of U_m .

By using the DC mode, U_m is served by BS_{*m*} and BS₀ simultaneously on a dedicated subcarrier, with the corresponding transmit powers denoted by P_m and P_{mm} , $1 \leq m \leq M$, respectively. Therefore, U_m 's achievable data rate, $1 \leq m \leq M$, is given by

$$\begin{aligned} R_m &= \log_2 \left(1 + \frac{\frac{\eta P_{mm}}{|\psi_m - \psi^{\text{Pin}}|^2}}{\frac{\eta P_m}{|\psi_m - \psi_m^{\text{BS}}|^2} + P_N} \right) \\ &+ \log_2 \left(1 + \frac{\eta P_m}{P_N |\psi_m - \psi_m^{\text{BS}}|^2} \right) \\ &= \log_2 \left(1 + \frac{\eta P_{mm}}{|\psi_m - \psi^{\text{Pin}}|^2} + \frac{\eta P_m}{P_N |\psi_m - \psi_m^{\text{BS}}|^2} \right), \end{aligned} \quad (2)$$

where ψ^{Pin} denotes the location of the pinching antenna, and the last step can be obtained directly from the capacity region of a multiple-access channel [30].

Because the newly arrived users, U_m , $1 \leq m \leq M$, are supported on dedicated subcarriers, the data rate of Cell₀'s existing user, U_0 , is the same as for the case without offloading, i.e., $R_0 = \log_2 \left(1 + \frac{\eta P_0}{P_N |\psi_0 - \psi^{\text{Pin}}|^2} \right)$, where P_0 denotes the transmit power.

Therefore, the overall transmit power minimization problem can be formulated as follows:

$$\min_{S_P, \psi^{\text{Pin}}} P_0 + \sum_{m=1}^M (P_m + P_{mm}) \quad (\text{P1a})$$

$$\text{s.t. } R_m \geq R, \quad 0 \leq m \leq M, \quad (\text{P1b})$$

- When complete offloading happens, where should the pinching antenna be placed?

Since on each subcarrier two users are served simultaneously, it is advantageous to use NOMA. In particular, on U_{0m} 's subcarrier, BS_0 first superimposes the signals for U_{0m} and U_m , and then broadcasts the mixture to the users. The adopted SIC decoding order, i.e., how the users carry out SIC, greatly affects the traffic offloading strategy, as discussed in the following two subsections. The optimal transmit powers and the pinching antenna location can be determined by comparing the outcomes of the optimization problems to be formulated for different SIC orders.

A. U_{0m} Carries Out SIC

If U_{0m} carries out SIC, U_{0m} can decode U_m 's signal with the following data rate:²

$$R_{0m}^m = \log_2 \left(1 + \frac{\frac{\eta P_{mm}}{|\psi_{0m} - \psi^{\text{Pin}}|^2}}{\frac{\eta P_{0m}}{|\psi_{0m} - \psi^{\text{Pin}}|^2} + P_N} \right), \quad (7)$$

where $\psi_{0m} = (x_{0m}, y_{0m}, 0)$ denotes U_{0m} 's location, P_{mm} denotes the transmit power assigned to U_m 's signal by BS_0 on U_{0m} 's subcarrier, and P_{0m} denotes the transmit power for U_{0m} 's signal.

Provided that the first step of SIC is successful, U_{0m} can then decode its own signal with the following data rate:

$$R_{0m} = \log_2 \left(1 + \frac{\eta P_{0m}}{P_N |\psi_{0m} - \psi^{\text{Pin}}|^2} \right). \quad (8)$$

Because the DC mode is used, U_m receives two signals, one from BS_0 on U_{0m} 's subcarrier and the other from BS_m on its own subcarrier. In particular, on U_{0m} 's subcarrier, U_m directly decodes its signal by treating U_{0m} 's signal as noise, and on its own subcarrier, there is no interference, which means that U_m 's data rate can be expressed as follows:

$$R_m = \log_2 \left(1 + \frac{\frac{\eta P_{mm}}{|\psi_m - \psi^{\text{Pin}}|^2}}{\frac{\eta P_{0m}}{|\psi_m - \psi^{\text{Pin}}|^2} + P_N} \right) + \log_2 \left(1 + \frac{\eta P_m}{P_N |\psi_m - \psi_m^{\text{BS}}|^2} \right). \quad (9)$$

Remark 1: In order to simplify the following optimization analysis, it is assumed that $R_{0m}^m \geq R_m$, which is equivalent to the following assumption:

$$|\psi_{0m} - \psi^{\text{Pin}}|^2 \leq |\psi_m - \psi^{\text{Pin}}|^2. \quad (10)$$

We note that the constraint in (10) means that the pinching antenna is placed closer to U_{0m} than U_m . This constraint is due to the adopted SIC decoding order, and will be employed by the resource allocation problem formulation.

²To reduce the system complexity, we assume that the users adopt the same SIC decoding order. Allowing the users to choose different SIC decoding orders can further improve the performance of pinching-antenna-assisted traffic offloading, which is beyond the scope of this paper due to space limitations but is an important direction for future research.

In particular, the overall transmit power minimization problem is formulated as follows:

$$\min_{S_P, \psi^{\text{Pin}}} \sum_{m=1}^M (P_{0m} + P_{mm} + P_m) \quad (P5a)$$

$$s.t. \quad \log_2 \left(1 + \frac{\eta P_{0m}}{P_N |\psi_{0m} - \psi^{\text{Pin}}|^2} \right) \geq R, \quad 1 \leq m \leq M, \quad (P5b)$$

$$\log_2 \left(1 + \frac{\frac{\eta P_{mm}}{|\psi_m - \psi^{\text{Pin}}|^2}}{\frac{\eta P_{0m}}{|\psi_m - \psi^{\text{Pin}}|^2} + P_N} \right) \quad (P5c)$$

$$+ \log_2 \left(1 + \frac{\eta P_m}{P_N |\psi_m - \psi_m^{\text{BS}}|^2} \right) \geq R, \quad 1 \leq m \leq M, \\ |\psi_{0m} - \psi^{\text{Pin}}|^2 < |\psi_m - \psi^{\text{Pin}}|^2, \quad 1 \leq m \leq M. \quad (P5d)$$

The above optimization problem can be solved by first determining the optimal transmit powers for a given pinching antenna location, and subsequently optimizing the antenna location, as shown in the following two subsections.

1) *Optimizing the transmit power for a given antenna location:* By assuming that the location of the pinching antenna is fixed, problem (P5) can be decomposed into the following M decoupled subproblems:

$$\min_{S_P^m} P_{0m} + P_{mm} + P_m \quad (P6a)$$

$$s.t. \quad (P5b), (P5c), \quad (P6b)$$

where $S_P^m = \{P_{0m}, P_{mm}, P_m\}$. Because the constraint $R_{0m}^m \geq R$ is removed, the optimization of U_{0m} 's signal power is decoupled from that of U_m 's signal powers. In particular, the optimal solution of P_{0m} can be obtained straightforwardly as follows: $P_{0m}^* = \epsilon |\psi_{0m} - \psi^{\text{Pin}}|^2$. Therefore, U_m 's signal powers can be optimized as follows:

$$\min_{P_{mm}, P_m} P_{mm} + P_m \quad (P7a)$$

$$s.t. \quad \log_2 \left(1 + \frac{P_{mm} g_{mm}}{P_{0m} g_{mm} + 1} \right) + \log_2 (1 + P_m g_m) \geq R, \quad (P7b)$$

where $g_m = \frac{\eta}{P_N |\psi_m - \psi_m^{\text{BS}}|^2}$ and $g_{mm} = \frac{\eta}{P_N |\psi_m - \psi^{\text{Pin}}|^2}$.

It is straightforward to show that problem (P7) is a convex optimization problem with respect to P_{mm} and P_m . The Lagrangian of problem (P7) is given by

$$\mathcal{L} = P_{mm} + P_m + \lambda_0 (R - \log_2 (1 + P_m g_m)) - \log_2 \left(1 + \frac{P_{mm} g_{mm}}{P_{0m} g_{mm} + 1} \right) - \lambda_1 P_{mm} - \lambda_2 P_m, \quad (11)$$

where λ_m , $0 \leq m \leq 2$, denote the Lagrangian multipliers corresponding to (P7b), $P_{mm} \geq 0$ and $P_m \geq 0$, respectively. By using the Lagrangian shown in (11) and also applying the Karush–Kuhn–Tucker (KKT) conditions, a closed-form expression for the optimal transmit power solution of problem (P7) can be obtained [32].

We note that problem (P7) is similar to the optimization problems obtained for power minimization in hybrid NOMA,

Because U_{0m} does not carry out SIC, it decodes its signal directly by treating U_m 's signal as noise, which means that U_{0m} 's achievable data rate is given by

$$R_{0m} = \log_2 \left(1 + \frac{\frac{\eta P_{0m}}{|\psi_{0m} - \psi^{\text{Pin}}|^2}}{\frac{\eta P_{mm}}{|\psi_{0m} - \psi^{\text{Pin}}|^2} + P_N} \right). \quad (19)$$

U_m can first decode U_{0m} 's signal with the following achievable data rate:

$$R_{0m}^m = \log_2 \left(1 + \frac{\frac{\eta P_{0m}}{|\psi_m - \psi^{\text{Pin}}|^2}}{\frac{\eta P_{mm}}{|\psi_m - \psi^{\text{Pin}}|^2} + P_N} \right). \quad (20)$$

Assuming that U_m can decode U_{0m} 's signal correctly, U_m can subtract U_{0m} 's signal and then decode its own signal with the following achievable data rate on U_{0m} 's subcarrier: $\log_2 \left(1 + \frac{\eta P_{mm}}{P_N |\psi_m - \psi^{\text{Pin}}|^2} \right)$. Since U_m receives two data streams from both BS_0 and BS_m , U_m 's overall achievable data rate is given by

$$R_m = \log_2 \left(1 + \frac{\eta P_{mm}}{P_N |\psi_m - \psi^{\text{Pin}}|^2} \right) + \log_2 \left(1 + \frac{\eta P_m}{P_N |\psi_m - \psi_m^{\text{BS}}|^2} \right). \quad (21)$$

Therefore, the considered total transmit power minimization problem can be formulated as follows:

$$\min_{S_P, \psi^{\text{Pin}}} \sum_{m=1}^M (P_{0m} + P_{mm} + P_m) \quad (P10a)$$

$$\text{s.t.} \quad \log_2 \left(1 + \frac{\frac{\eta P_{0m}}{|\psi_{0m} - \psi^{\text{Pin}}|^2}}{\frac{\eta P_{mm}}{|\psi_{0m} - \psi^{\text{Pin}}|^2} + P_N} \right) \geq R, \quad 1 \leq m \leq M, \quad (P10b)$$

$$\log_2 \left(1 + \frac{\eta P_{mm}}{P_N |\psi_m - \psi^{\text{Pin}}|^2} \right) \quad (P10c)$$

$$+ \log_2 \left(1 + \frac{\eta P_m}{P_N |\psi_m - \psi_m^{\text{BS}}|^2} \right) \geq R, \quad 1 \leq m \leq M,$$

$$|\psi_{0m} - \psi^{\text{Pin}}|^2 \geq |\psi_m - \psi^{\text{Pin}}|^2, \quad 1 \leq m \leq M. \quad (P10d)$$

Remark 4: Similar to the case considered in the previous section, it is assumed that U_m can carry out SIC successfully, i.e., $R_{0m}^m \geq R_{0m}$, which leads to the constraint shown in (P10d). Similar to problem (P5), problem (P10) can be solved in two stages, as shown in the following subsections.

1) *Optimizing the transmit power for a given antenna location:* For a given pinching antenna location, problem (P10) can be decomposed into the following M decoupled subproblems:

$$\min_{S_m^P} P_{0m} + P_{mm} + P_m \quad (P11a)$$

$$\text{s.t.} \quad (2^R - 1) g_{0m} P_{mm} - g_{0m} P_{0m} + (2^R - 1) \leq 0, \quad (P11b)$$

$$R - \log_2 (1 + g_{mm} P_{mm}) - \log_2 (1 + g_m P_m) \leq 0, \quad (P11c)$$

where $g_{0m} = \frac{\eta}{P_N |\psi_{0m} - \psi^{\text{Pin}}|^2}$.

Unlike problem (P5) or the problems in [33], for problem (P11), the optimization of U_{0m} 's transmit power, P_m , is inherently coupled with that of P_m and P_{mm} , and therefore it cannot be solved separately. Nevertheless, the optimal transmit powers can be obtained in closed-form as shown in the following lemma.

Lemma 1. *The optimal solution of problem (P11) can be expressed as follows:*

$$P_{mm} = \begin{cases} \sqrt{\frac{1}{g_{mm} g_m}} - \frac{1}{g_{mm}}, & \text{Case I} \\ 0, & \text{Case II} \\ \frac{2^R - 1}{g_{mm}}, & \text{Case III} \end{cases}, \quad (22)$$

$$P_{0m} = \begin{cases} (2^R - 1) P_{mm} + \frac{2^R - 1}{g_{0m}}, & \text{Case I} \\ \frac{2^R - 1}{g_{0m}}, & \text{Case II} \\ \frac{(2^R - 1)^2}{g_{mm}} + \frac{2^R - 1}{g_{0m}}, & \text{Case III} \end{cases}, \quad (23)$$

$$P_m = \begin{cases} \frac{2^R}{\sqrt{g_m g_{mm}}} - \frac{1}{g_m}, & \text{Case I} \\ \frac{2^R - 1}{g_m}, & \text{Case II} \\ 0, & \text{Case III} \end{cases}, \quad (24)$$

where the conditions for the three cases are given by

$$\begin{cases} \text{Case I:} & 1 < \frac{g_{mm}}{g_m} < 2^{2R} \\ \text{Case II:} & \frac{g_{mm}}{g_m} \leq 1 \\ \text{Case III:} & \frac{g_{mm}}{g_m} \geq 2^{2R} \end{cases}. \quad (25)$$

Proof. See Appendix A. \square

2) *Optimizing the pinching antenna location:* Similar to the previous section, the case with complete traffic offloading will be focused on here, since it leads to a reduction of the traffic and an increase of the available bandwidth in Cell_m , $1 \leq m \leq M$.

By using the optimality condition for Case III shown in Lemma 1, problem (P10) can be expressed as follows:

$$\min_{\psi^{\text{Pin}}} \sum_{m=1}^M (P_{0m} + P_{mm}) \quad (P12a)$$

$$\text{s.t.} \quad |\psi_m - \psi_m^{\text{BS}}|^2 \geq 2^{2R} |\psi_m - \psi^{\text{Pin}}|^2, \quad 1 \leq m \leq M, \quad (P12b)$$

$$|\psi_{0m} - \psi^{\text{Pin}}|^2 \geq |\psi_m - \psi^{\text{Pin}}|^2, \quad 1 \leq m \leq M, \quad (P12c)$$

where the constraint in (P12b) is due to the fact that the complete offloading case is focused on, and the constraint in (P12c) is due to the adopted SIC decoding order.

By using the closed-form expressions in Lemma 1, the objective function of problem (P12) can be expressed as the following explicit function of the pinching antenna location:

$$\begin{aligned} P_{0m} + P_{mm} &= \frac{2^R (2^R - 1)}{g_{mm}} + \frac{2^R - 1}{g_{0m}} \\ &= 2^R \epsilon |\psi_m - \psi^{\text{Pin}}|^2 + \epsilon |\psi_{0m} - \psi^{\text{Pin}}|^2. \end{aligned} \quad (26)$$

By using the expression for the total transmit power shown in (26), problem (P12) can be expressed as follows:

$$\min_{\psi^{\text{Pin}}} \sum_{m=1}^M \left(2^R \epsilon |\psi_m - \psi^{\text{Pin}}|^2 + \epsilon |\psi_{0m} - \psi^{\text{Pin}}|^2 \right) \quad (P13a)$$

$$s.t. \quad (P12b), (P12c). \quad (P13b)$$

Problem (P13) can be further expressed as the following convex form:

$$\min_{x^{\text{Pin}}} \sum_{m=1}^M \left(2^R (x^{\text{Pin}} - x_m)^2 + (x^{\text{Pin}} - x_{0m})^2 \right) \quad (P14a)$$

$$s.t. \quad 2^{2R} (x^{\text{Pin}} - x_m)^2 \leq d_{3m}, \quad 1 \leq m \leq M, \quad (P14b)$$

$$2(x_m - x_{0m})x^{\text{Pin}} > d_{2m}, \quad 1 \leq m \leq M, \quad (P14c)$$

where $d_{3m} = |\psi_m - \psi_m^{\text{BS}}|^2 - 2^{2R} (y^{\text{Pin}} - y_m)^2 - 2^{2R} d^2$. It is straightforward to verify that problem (P14) is a convex optimization problem, and hence it can be solved efficiently by off-the-shelf optimization solvers.

After the optimal solutions for problems (P9) and (P12) are obtained, the minimal transmit power can be determined by comparing the objective values of the two problems.

C. A Special Case Study

This subsection focuses on the special case with two cells, i.e., BS₁ offloads U₁'s traffic to BS₀. Recall that two optimization problems have been formulated for the cases with different SIC decoding orders. As can be seen from (P8) and (P12), there are two constraints for each of the formulated problems, one for the optimality of the complete offloading strategy and the other due to the adopted SIC decoding order. In this section, we assume that the distance between U₁ and BS₁ is so large that the constraints in (P8b) and (P12b) always hold for any choice of x^{Pin} , i.e., complete offloading is always preferred. For example, if BS₁ is a macro base station, it is very likely that the distance between U₁ and BS₁ is much larger than the distances between the user and the pinching antenna of the small cell base station.

With the aforementioned assumptions, a concise closed-form expression can be obtained for the optimal antenna location. In particular, denote the strong and weak users by U_s and U_w, respectively. In particular, if $|y_{01}| \leq |y_1|$, U₀₁ is the strong user, and U₁ is the weak user, i.e., U_s = U₀₁ and U_w = U₁, otherwise U_s = U₁ and U_w = U₀₁. The locations of U_s and U_w are denoted by $(x_s, y_s, 0)$ and $(x_w, y_w, 0)$, respectively. For the waveguide deployment illustrated in Fig. 2(b), we assume that $y^{\text{Pin}} = 0$. With the above assumptions, the optimal pinching antenna location and the minimal transmit power are provided in the following lemma.

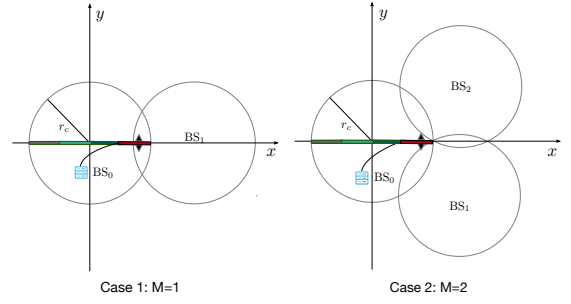


Fig. 3. Illustration of the two considered network topologies. In Case I, there are two cells, i.e., $M = 1$, where both U₀ and U₁ are uniformly distributed in the overlapping area between the two cells. In Case II, there are three cells, i.e., $M = 2$, where U_m is uniformly distributed in the overlapping area between Cell₀ and Cell_m, $m \in \{1, 2\}$. For the strategy considered in Section III, there is a single user (U₀) served by the pinching antenna in Cell₀, and the location of U₀ is generated in the same manner as in Case I. For the strategy considered in Section IV, each offloaded user, U_m, is paired with an existing user (U_{0m}), where U_{0m} and U_m are uniformly distributed in the same overlapping area.

Lemma 2. For the considered special case, the minimal transmit power can be achieved by asking U_s to carry out SIC, and the minimal transmit power is given by

$$P^{\text{all}*} = \frac{\epsilon 2^R}{2^R + 1} (x_s - x_w)^2 + \epsilon (2^R y_s^2 + y_w^2) + \epsilon (2^R + 1) d^2, \quad (27)$$

and the optimal pinching antenna location is given by

$$x^{\text{Pin}*} = \frac{(2^R x_s + x_w)}{2^R + 1}. \quad (28)$$

Proof. See Appendix B. \square

Remark 5: Lemma 2 shows that, for the considered two-cell special case, multiple resource allocation problems based on different SIC decoding orders are not needed. In particular, there is a dominant SIC order, which leads to the minimal overall transmit power. Furthermore, the closed-form solution shown in (28) reveals that the optimal antenna location is a function of the projections of the users' positions onto the waveguide only. However, we note that the distances between the users and the waveguide, i.e., y_m and y_{0m} , still affect the optimal antenna location by determining which SIC decoding order is dominant.

V. NUMERICAL RESULTS

In this section, the performance of pinching-antenna-assisted traffic offloading is evaluated by using computer simulations. The network topologies shown in Fig. 3 are used for the conducted simulations. Throughout this section, it is assumed that $f_c = 28$ GHz, $d = 3$ m, $N = 4$, and the noise power is -70 dBm. The cell radius is denoted by r_c , and the distance between BS₀ and BS_m, $1 \leq m \leq M$, is denoted by $r_d = \sqrt{3}r_c$ ³. The waveguide in Cell₀ is placed on the x axis of the plane shown in Fig. 3, and its length is $2r_c$. Furthermore, as illustrated in Fig. 2(b), the rightmost waveguide segment is the focus of interest, and hence $x_m \geq \frac{N-2}{N}r_c$, $0 \leq m \leq M$, i.e., the scheduled users should not fall to the left-hand side of the considered segment.

³The choice of $r_d = \sqrt{3}r_c$ ensures that there is a single intersection between the three circles in Fig. 3.

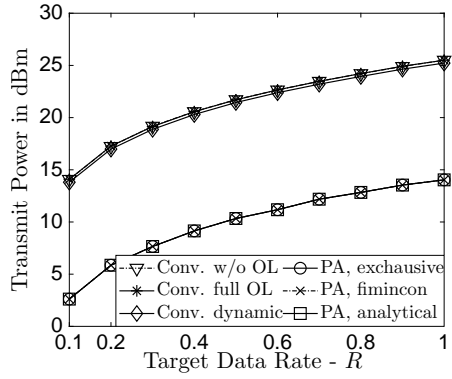
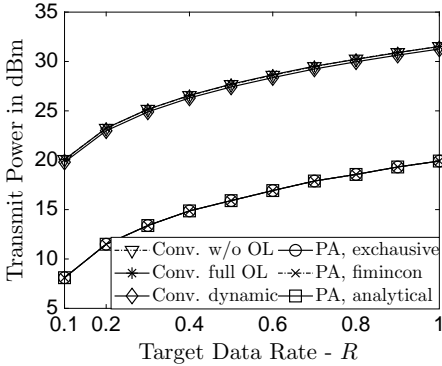
(a) Case I with $r_c = 40$ m(b) Case I with $r_c = 80$ m

Fig. 4. Impact of pinching antennas on the transmit power for the considered traffic offloading schemes, where Case I is focused on and the scenario in Section III is considered.

Figs. 4, 5, and 6 focus on the case in which U_m keeps using its subcarrier in $Cell_m$, i.e., the scenario considered in Section III. In particular, Fig. 4 compares the transmit powers required by different traffic offloading schemes in order to achieve the target data rate R , where Case I shown in Fig. 3 is focused on. In order to facilitate the performance analysis, three types of conventional-antenna-based schemes are used for benchmarking, where the first one does not employ traffic offloading, the second one forces BS_0 to serve U_m , $m \in \{1, \dots, M\}$, and the third one is based on dynamic traffic offloading to realize the minimum between the transmit powers achieved by the first two benchmarking schemes. As can be seen from the figure, the use of pinching antennas can significantly reduce the transmit power for traffic offloading. For example, for Case I with $r_c = 40$ m, the performance gain of the pinching-antenna scheme over the conventional ones is more than 10 dBm, i.e., the use of pinching antennas can reduce the transmit power by more than a factor of 10. For the optimization problem shown in (P3), the optimal solution can be obtained by applying an exhaustive search, an off-the-shelf optimization solver, such as Matlab `fmincon`, as well as in a closed-form expression provided in (6) for the special case of $M = 1$. Fig. 4 shows that the performance achieved with the analytical solution is identical to that obtained with `fmincon` and an exhaustive search, which verifies the optimality of the obtained analytical result shown in (6).

Fig. 5 focuses on Case II, i.e., there are three cells in the network and the users from $Cell_1$ and $Cell_2$ are offloaded and served by BS_0 . Consistent with Fig. 4, Fig. 5 demonstrates that the use of pinching antennas can significantly reduce the transmit power required for traffic offloading. However, com-

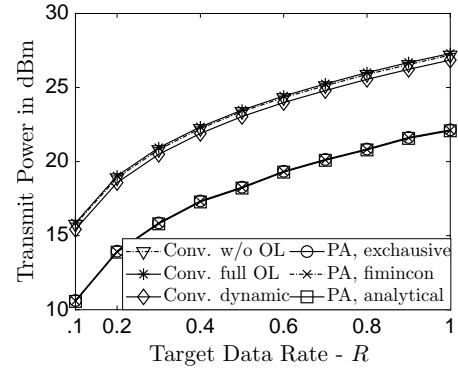
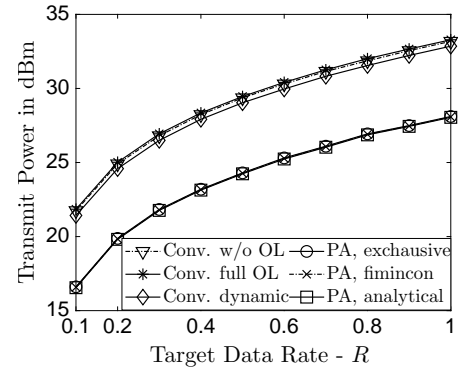
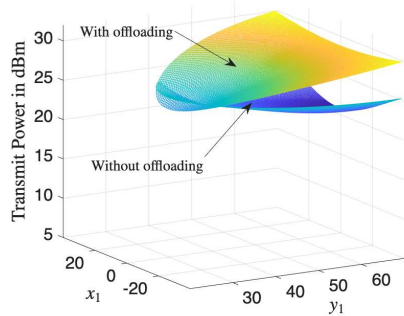
(a) Case II with $r_c = 40$ m(b) Case II with $r_c = 80$ m

Fig. 5. Impact of pinching antennas on the transmit power for the considered traffic offloading schemes, where Case II is focused on and the scenario in Section III is considered.

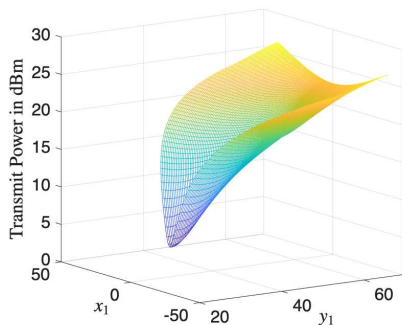
paring Fig. 5 and Fig. 4, one can observe that the performance gain of pinching-antenna systems over conventional-antenna systems decreases by increasing M . The reason for this performance degradation is that a single antenna is activated to serve multiple users from the $M + 1$ cells. For the case with a small M , the location of the pinching antenna is tailored to the served users; however, with a large M , the adopted antenna location becomes a compromise choice, i.e., the adopted location might not be ideal for any individual user.

Fig. 6 illustrates the performance gain of pinching-antenna systems over conventional-antenna systems with deterministic user locations. The key observation from Fig. 6 is that the performance gain of pinching antennas depends on U_1 's location. In particular, if U_1 is a cell edge user, the performance gain of pinching-antenna systems over conventional-antenna systems is enormous. The reason for this significant performance gain is that with conventional antennas, a cell-edge user is far away from both BS_0 and BS_1 . Therefore, the user has to be served with a large transmit power, with or without traffic offloading. However, due to its flexibility, the pinching antenna can be placed close to the cell-edge user, which means that the user can be served by BS_0 with low transmit power.

Figs. 7, 8, and 9 focus on the scenario in which U_m releases its subcarrier in $Cell_m$, i.e., the scenario considered in Section IV. The two network topologies shown in Fig. 3 are still used. Fig. 7 focuses on Case I, where there are two cells. Consistent with the previous results, Fig. 7 shows that using pinching antennas significantly reduces the transmit power, which is due to the fact that BS_0 can place its pinching antenna close to the user to be offloaded from $Cell_1$ to $Cell_0$. We note that for the special case of $M = 1$, closed-form expressions for the



(a) Conventional antennas



(b) Pinching antennas

Fig. 6. Impact of pinching antennas on the transmit power for the considered traffic offloading schemes, where Case I is focused on and the scenario in Section III is considered. Unlike Fig. 4, the location of U_0 is fixed at the middle of the considered segment, i.e., $(\frac{N-1}{N}r_c, 0, 0)$, and U_1 is assumed to be within a left-hand-side semicircular region of radius r_c and its center at BS_1 , where $r_c = 40$ m.

optimal solutions of power allocation and antenna placement can be obtained as shown in Lemma 2. The fact that the analytical solution yields the same performance as the schemes based on an exhaustive search and optimization solvers verifies the optimality of the analytical solution.

Fig. 8 focuses on Case II, where there are three cells. While pinching-antenna systems can still outperform the benchmarking schemes, the performance gain of pinching antennas over conventional antennas reduces by increasing M , a phenomenon consistent with the previously presented simulation results. Fig. 9 shows the performance gain of pinching-antenna systems over conventional-antenna systems for deterministic user locations. Similar to Fig. 6, Fig. 9 shows that users close to the cell boundary benefit significantly from traffic offloading in pinching-antenna systems. Unlike Figs. 4-6, Figs. 7-9 show that if conventional antennas are used, the scheme with complete traffic offloading suffers the worst performance, which means that with conventional antennas, traffic offloading almost never happens. However, the use of pinching antennas makes complete traffic offloading a preferred choice, which is important in practice. Take the scenario considered in Section III as an example. Complete traffic offloading is particularly meaningful, where the use of pinching antennas ensures that U_m , $1 \leq m \leq M$, can be offloaded to $Cell_0$ and their bandwidth in $Cell_m$ can be released to support additional users. In addition, pinching-antenna assisted traffic offloading requires lower transmit power and hence supports greener communications, compared to the benchmarking schemes.

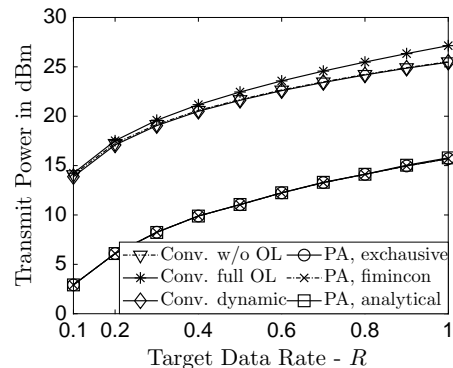
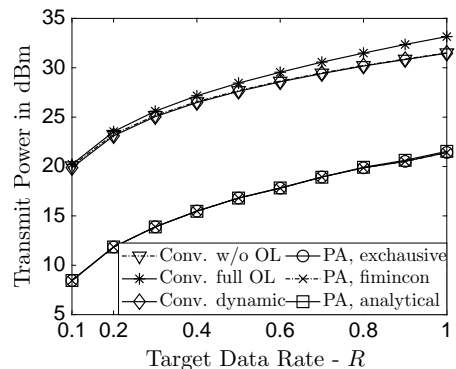
(a) Case I with $r_c = 40$ m(b) Case I with $r_c = 80$ m

Fig. 7. Impact of pinching antennas on the transmit power for the considered traffic offloading schemes, where Case I is focused on and the scenario in Section IV is considered.

VI. CONCLUSIONS

In this paper, the key features of pinching antennas, i.e., establishing strong connections between transceivers and making the physical boundaries of wireless cells reconfigurable, have been used to facilitate traffic offloading. An overall transmit power minimization problem has been formulated, where the optimal transmit powers and antenna locations have been obtained. Our analytical and simulation results demonstrate that the use of pinching antennas can efficiently support traffic offloading, achieve low energy consumption, and realize balanced cell resource utilization.

In this paper, it was assumed that only a single cell is equipped with a pinching-antenna system. The application of pinching antennas to general multi-cell scenarios, such as cloud radio access networks (C-RAN), fog radio access networks (F-RAN), and cell-free massive multiple-input multiple-output (MIMO) networks, is an important direction for future research [34]–[37].

APPENDIX A PROOF FOR LEMMA 1

Problem (P11) is a convex optimization problem, and hence its optimal solution can be obtained based on the KKT conditions. The Lagrangian of problem (P11) is given by

$$\begin{aligned} \mathcal{L} = & P_{0m} + P_{mm} + P_m - \lambda_1 P_{0m} - \lambda_2 P_{mm} - \lambda_3 P_m \quad (29) \\ & + \lambda_4 ((2^R - 1) g_{0m} P_{mm} - g_{0m} P_{0m} + (2^R - 1)) \\ & + \lambda_5 (R - \log_2(1 + g_{mm} P_{mm}) - \log_2(1 + g_m P_m)), \end{aligned}$$

where λ_m , $1 \leq m \leq 5$, denote the Lagrangian multipliers.

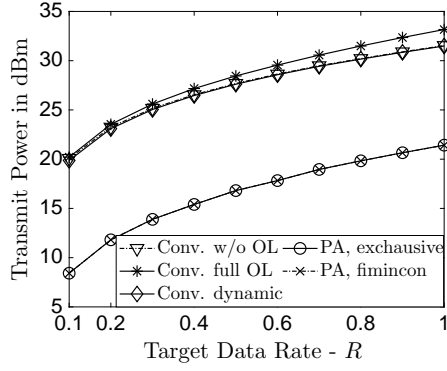
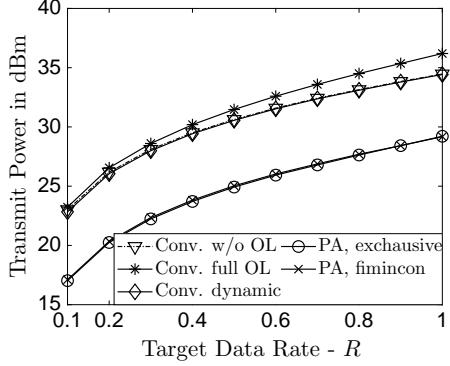
(a) Case II with $r_c = 40$ m(b) Case II with $r_c = 80$ m

Fig. 8. Impact of pinching antennas on the transmit power for the considered traffic offloading schemes, where Case II is focused on and the scenario in Section IV is considered.

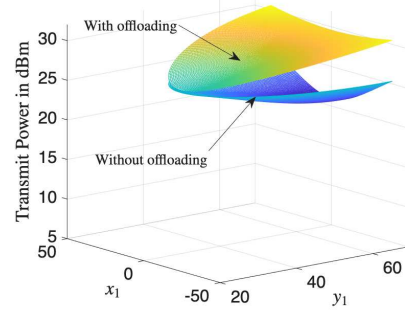
The corresponding KKT conditions for problem (P11) are given by

$$\begin{cases} 1 - \lambda_1 - \lambda_4 g_{0m} = 0 \\ 1 - \lambda_2 + \lambda_4 (2^R - 1) g_{0m} - \frac{g_{mm} \lambda_5}{(1 + g_{mm} P_{mm}) \log 2} = 0 \\ 1 - \lambda_3 - \frac{g_m \lambda_5}{(1 + g_m P_m) \log 2} = 0 \\ \lambda_4 ((2^R - 1) g_{0m} P_{mm} - g_{0m} P_{0m} + (2^R - 1)) = 0 \\ \lambda_5 (R - \log_2 (1 + g_{mm} P_{mm}) - \log_2 (1 + g_m P_m)) = 0 \\ \lambda_1 P_{0m} = 0, \lambda_2 P_{mm} = 0, \lambda_3 P_m = 0 \\ (2^R - 1) g_{0m} P_{mm} - g_{0m} P_{0m} + (2^R - 1) \leq 0 \\ R - \log_2 (1 + g_{mm} P_{mm}) - \log_2 (1 + g_m P_m) \leq 0 \\ P_{mm} \geq 0, P_m \geq 0, P_{0m} \geq 0 \end{cases}, \quad (30)$$

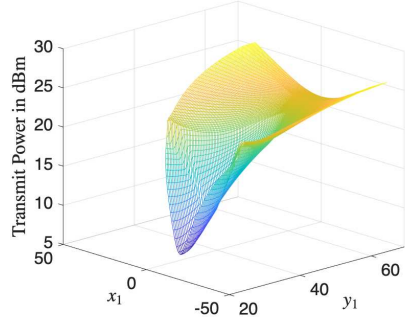
where $\log(\cdot)$ denotes the natural logarithm. It is straightforward to show that $P_{0m} \neq 0$, which means that $\lambda_1 = 0$. The fact that $\lambda_1 = 0$ leads to the conclusions that $\lambda_4 = \frac{1}{g_{0m}}$ and $(2^R - 1) g_{0m} P_{mm} - g_{0m} P_{0m} + (2^R - 1) = 0$. The discussions in Section III lead to the intuition that there could be three cases, which correspond to U_m 's offloading strategies and hence are analyzed separately in the following.

1) $P_m \neq 0$ and $P_{mm} \neq 0$: In this case, U_m is simultaneously served by both BS_m and BS_0 . The KKT conditions shown in (39) can be simplified as follows:

$$\begin{cases} 2^R - \frac{g_{mm} \lambda_5}{(1 + g_{mm} P_{mm}) \log 2} = 0, 1 - \frac{g_m \lambda_5}{(1 + g_m P_m) \log 2} = 0 \\ (2^R - 1) g_{0m} P_{mm} - g_{0m} P_{0m} + (2^R - 1) = 0 \\ \lambda_5 (R - \log_2 (1 + g_{mm} P_{mm}) - \log_2 (1 + g_m P_m)) = 0 \\ \lambda_1 = 0, \lambda_2 = 0, \lambda_3 = 0, \lambda_4 = \frac{1}{g_{0m}} \\ R - \log_2 (1 + g_{mm} P_{mm}) - \log_2 (1 + g_m P_m) \leq 0 \\ P_{mm} \geq 0, P_m \geq 0, P_{0m} \geq 0 \end{cases}. \quad (31)$$



(a) Conventional antennas



(b) Pinching antennas

Fig. 9. Impact of pinching antennas on the transmit power for the considered traffic offloading schemes, where Case I is focused on and the scenario in Section IV is considered. The same system parameter values as in Fig. 6 are used.

It is straightforward to show that $\lambda_5 \neq 0$, which means the three transmit power solutions can be obtained from the following linear equations:

$$\begin{cases} g_{mm} (1 + g_m P_m) = g_m 2^R (1 + g_{mm} P_{mm}) \\ (2^R - 1) g_{0m} P_{mm} - g_{0m} P_{0m} + (2^R - 1) = 0 \\ R - \log_2 (1 + g_{mm} P_{mm}) - \log_2 (1 + g_m P_m) = 0 \end{cases}, \quad (32)$$

which leads to the following solutions:

$$\begin{aligned} P_{mm} &= \frac{1}{g_{mm}} \left(\sqrt{\frac{g_{mm}}{g_m}} - 1 \right), & P_m &= \frac{1}{g_m} \left(2^R \sqrt{\frac{g_m}{g_{mm}}} - 1 \right), \\ P_{0m} &= \frac{2^R - 1}{g_{0m}} (g_{0m} P_{mm} + 1). \end{aligned} \quad (33)$$

The solutions in (33) yields $\lambda_5 = \frac{2^R \log 2}{\sqrt{g_m g_{mm}}} \geq 0$, and therefore, the condition for the solutions in (33) to be optimal is $P_{mm} > 0$ and $P_m > 0$, i.e.,

$$\sqrt{\frac{g_{mm}}{g_m}} - 1 > 0, \quad 2^R \sqrt{\frac{g_m}{g_{mm}}} - 1 > 0, \quad (34)$$

which means

$$1 < \frac{g_{mm}}{g_m} < 2^{2R}. \quad (35)$$

2) $P_m = 0$ and $P_{mm} \neq 0$: This case corresponds to the scenario, where U_m is completely offloaded from $Cell_m$ to

Cell₀. In this case, the KKT conditions can be simplified as follows:

$$\begin{cases} 2^R - \frac{g_{mm}\lambda_5}{(1+g_{mm}P_{mm})\log 2} = 0 \\ 1 - \lambda_3 - \frac{g_m\lambda_5}{\log 2} = 0 \\ (2^R - 1)g_{0m}P_{mm} - g_{0m}P_{0m} + (2^R - 1) = 0 \\ \lambda_5(R - \log_2(1 + g_{mm}P_{mm})) = 0 \\ \lambda_1 = 0, \lambda_2 = 0, P_m = 0, \lambda_4 = \frac{1}{g_{0m}} \\ R - \log_2(1 + g_{mm}P_{mm}) \leq 0 \\ P_{mm} \geq 0, P_m = 0, P_{0m} \geq 0 \end{cases} \quad (36)$$

It is straightforward to show that $\lambda_5 \neq 0$, which leads to the following conclusions:

$$\begin{cases} P_{0m} = (2^R - 1) \left[(2^R - 1) \frac{1}{g_{mm}} + \frac{1}{g_{0m}} \right] \\ P_{mm} = \frac{2^R - 1}{g_{mm}}, P_m = 0 \\ \lambda_1 = 0, \lambda_2 = 0, P_m = 0, \lambda_4 = \frac{1}{g_{0m}} \\ \lambda_5 = \frac{2^{2R} \log 2}{g_{mm}}, \lambda_3 = 1 - g_m \frac{2^{2R}}{g_{mm}} \end{cases} \quad (37)$$

Therefore, the condition for the optimality of this case is given by

$$\lambda_3 \geq 0 \implies \frac{g_{mm}}{g_m} \geq 2^{2R}. \quad (38)$$

3) $P_m \neq 0$ and $P_{mm} = 0$: This case corresponds to the scenario where U_m chooses to stay in Cell_m. In this case, the KKT conditions can be simplified as follows:

$$\begin{cases} 2^R - \lambda_2 - \frac{g_{mm}\lambda_5}{\log 2} = 0 \\ 1 - \frac{g_m\lambda_5}{(1+g_mP_m)\log 2} = 0 \\ -g_{0m}P_{0m} + (2^R - 1) = 0 \\ \lambda_5(R - \log_2(1 + g_mP_m)) = 0 \\ \lambda_1 = 0, \lambda_2 P_{mm} = 0, \lambda_3 = 0, \lambda_4 = \frac{1}{g_{0m}} \\ R - \log_2(1 + g_mP_m) \leq 0 \\ P_{mm} = 0, P_m \geq 0, P_{0m} \geq 0 \end{cases} \quad (39)$$

By using the fact that $\lambda_5 \neq 0$, the optimal solution can be obtained as follows:

$$\begin{cases} P_{0m} = \frac{2^R - 1}{g_{0m}}, P_m = \frac{2^R - 1}{g_m}, P_{mm} = 0 \\ \lambda_1 = 0, \lambda_3 = 0, \lambda_4 = \frac{1}{g_{0m}} \\ \lambda_2 = 2^R \left(1 - \frac{g_{mm}}{g_m} \right), \lambda_5 = \frac{2^R \log 2}{g_m} \end{cases} \quad (40)$$

Therefore, the condition for the optimality of this case is given by

$$\lambda_2 \geq 0 \implies \frac{g_{mm}}{g_m} \leq 1. \quad (41)$$

By combining (33), (35), (37), (38), (40), (41), the proof for Lemma 1 is complete.

APPENDIX B PROOF FOR LEMMA 2

The lemma can be proved by studying the following two cases with different SIC decoding orders.

1) U_{01} carries out SIC: For the considered special case, the constraint for complete offloading shown in (P9b) is assumed to be always satisfied and hence can be omitted. To facilitate the analysis of the optimal pinching antenna location, (P9c) is first ignored, and hence problem (P9) can be simplified as follows:

$$\min_{x^{\text{Pin}}} 2^R (x_{0m} - x^{\text{Pin}})^2 + (x_m - x^{\text{Pin}})^2. \quad (P15a)$$

Therefore, the optimal solution for the pinching antenna location is given by

$$x^{\text{Pin}*} = \frac{2^R x_{0m} + x_m}{2^R + 1}, \quad (42)$$

which means that the minimal transmit power is given by

$$\begin{aligned} P^{\text{all}} &= \epsilon 2^R \left[\left(x_{01} - \frac{(2^R x_{01} + x_1)}{(2^R + 1)} \right)^2 + y_{01}^2 + d^2 \right] \\ &\quad + \epsilon \left[\left(x_1 - \frac{(2^R x_{01} + x_1)}{(2^R + 1)} \right)^2 + y_1^2 + d^2 \right] \\ &= \epsilon \frac{2^R}{2^R + 1} (x_{01} - x_1)^2 + \epsilon 2^R y_{01}^2 \\ &\quad + \epsilon y_1^2 + \epsilon (2^R + 1) d^2. \end{aligned} \quad (43)$$

In the following, we will show that the obtained optimal solution satisfies constraint (P9c) (or equivalently (P8c)), if $|y_{01}| \leq |y_1|$. In particular, with the optimal solution shown in (42), the difference between $|\psi_{01} - \psi^{\text{Pin}}|^2$ and $|\psi_1 - \psi^{\text{Pin}}|^2$ shown in (P8c) can be expressed as follows:

$$\begin{aligned} &|\psi_{01} - \psi^{\text{Pin}}|^2 - |\psi_1 - \psi^{\text{Pin}}|^2 \quad (44) \\ &= \left[\left(x_{01} - \frac{(2^R x_{01} + x_1)}{(2^R + 1)} \right)^2 + y_{01}^2 + d^2 \right] \\ &\quad - \left[\left(x_1 - \frac{(2^R x_{01} + x_1)}{(2^R + 1)} \right)^2 + y_1^2 + d^2 \right] \\ &= \left[\left(\frac{(x_{01} - x_1)}{(2^R + 1)} \right)^2 + y_{01}^2 + d^2 \right] \\ &\quad - \left[2^{2R} \left(\frac{(x_1 - x_{01})}{(2^R + 1)} \right)^2 + y_1^2 + d^2 \right] \\ &= -\frac{2^R - 1}{2^R + 1} (x_{01} - x_1)^2 + y_{01}^2 - y_1^2. \end{aligned}$$

Therefore, the condition $|y_{01}| \leq |y_1|$ guarantees the constraint shown in (P8c), i.e., $|\psi_{01} - \psi^{\text{Pin}}|^2 \leq |\psi_1 - \psi^{\text{Pin}}|^2$.

2) U_1 carries out SIC: Again, to facilitate the proof, the constraint shown in (P14c) is ignored first. Since the constraint of (P14b) is assumed to be satisfied for the considered special case, problem (P14) can be simplified as follows:

$$\min_{x^{\text{Pin}}} 2^R (x^{\text{Pin}} - x_1)^2 + (x^{\text{Pin}} - x_{01})^2, \quad (P16a)$$

whose optimal solution is given by

$$x^{\text{Pin}} = \frac{2^R x_1 + x_{01}}{2^R + 1}. \quad (45)$$

By using the above pinching antenna location, the minimal transmit power for this case is given by

$$\begin{aligned}
P^{\text{all}} &= \epsilon 2^R \left(x_1 - \frac{2^R x_1 + x_{01}}{2^R + 1} \right)^2 + \epsilon 2^R y_1^2 + \epsilon 2^R d^2 \\
&+ \epsilon \left(x_{01} - \frac{2^R x_1 + x_{01}}{2^R + 1} \right)^2 + \epsilon y_{01}^2 + \epsilon d^2 \\
&= \epsilon \frac{2^R}{2^R + 1} (x_{01} - x_1)^2 + \epsilon 2^R y_1^2 + \epsilon y_{01}^2 + \epsilon (2^R + 1) d^2.
\end{aligned} \quad (46)$$

In order to show that the obtained optimal solution satisfies the constraint shown in (P14c), we note that with the optimal pinching antenna location, the difference between the distances, $|\psi_{01} - \psi^{\text{Pin}}|^2$ and $|\psi_1 - \psi^{\text{Pin}}|^2$ can be expressed as follows:

$$\begin{aligned}
&|\psi_{01} - \psi^{\text{Pin}}|^2 - |\psi_1 - \psi^{\text{Pin}}|^2 \\
&= \left(\frac{2^R x_1 + x_{01}}{2^R + 1} - x_{01} \right)^2 + y_{01}^2 - \left(\frac{2^R x_1 + x_{01}}{2^R + 1} - x_1 \right)^2 - y_1^2 \\
&= \frac{2^R - 1}{2^R + 1} (x_1 - x_{01})^2 + y_{01}^2 - y_1^2.
\end{aligned} \quad (47)$$

Therefore, if $|y_{01}| > |y_1|$, the constraint shown in (P14c) is satisfied.

By combining (42), (43), (45), and (46), the concise expressions shown in Lemma 2 can be obtained and the proof is complete.

REFERENCES

- [1] X. You, C. Wang, J. Huang *et al.*, "Towards 6G wireless communication networks: Vision, enabling technologies, and new paradigm shifts," *Sci. China Inf. Sci.*, vol. 64, no. 110301, pp. 1–74, Feb. 2021.
- [2] M. D. Renzo, M. Debbah, D.-T. Phan-Huy, A. Zappone, M.-S. Alouini, C. Yuen, V. Sciancalepore, G. C. Alexandropoulos, J. Hoydis, H. Gacanin, J. de Rosny, A. Bounceu, G. Lerosey, and M. Fink, "Smart radio environments empowered by AI reconfigurable meta-surfaces: An idea whose time has come," *EURASIP J. on Wirel. Com. Netw.*, vol. 129, pp. 1–20, May 2019.
- [3] Q. Wu and R. Zhang, "Intelligent reflecting surface enhanced wireless network via joint active and passive beamforming," *IEEE Trans. Wirel. Commun.*, vol. 18, no. 11, pp. 5394–5409, Nov. 2019.
- [4] L. Zhu, W. Ma, and R. Zhang, "Modeling and performance analysis for movable antenna enabled wireless communications," *IEEE Trans. Wireless Commun.*, vol. 23, no. 6, pp. 6234–6250, Jun. 2024.
- [5] K.-K. Wong, A. Shojaifard, K.-F. Tong, and Y. Zhang, "Fluid antenna systems," *IEEE Trans. Wireless Commun.*, vol. 20, no. 3, pp. 1950–1962, Mar. 2021.
- [6] A. Fukuda, H. Yamamoto, H. Okazaki, Y. Suzuki, and K. Kawai, "Pinching antenna - using a dielectric waveguide as an antenna," *NTT DOCOMO Technical J.*, vol. 23, no. 3, pp. 5–12, Jan. 2022.
- [7] Z. Ding, R. Schober, and H. V. Poor, "Flexible-antenna systems: A pinching-antenna perspective," *IEEE Trans. Commun.*, vol. 73, no. 10, pp. 9236–9253, Oct. 2025.
- [8] Y. Xu, J. Cui, Y. Zhu, Z. Ding, T.-H. Chang, R. Schober, V. W. S. Wong, O. A. Dobre, G. K. Karagiannidis, H. V. Poor, and X. You, "Generalized pinching-antenna systems: A tutorial on principles, design strategies, and future directions," *IEEE Commun. Surveys Tuts.*, vol. 28, pp. 5872–5908, 2026.
- [9] Z. Wang, C. Ouyang, X. Mu, Y. Liu, and Z. Ding, "Modeling and beamforming optimization for pinching-antenna systems," *IEEE Trans. Commun.*, vol. 73, no. 12, pp. 13 904–13 919, Dec. 2025.
- [10] C. Ouyang, H. Jiang, Z. Wang, Y. Liu, and Z. Ding, "Uplink and downlink communications in segmented waveguide-enabled pinching-antenna systems (SWANs)," *IEEE Trans. Commun.*, vol. 74, pp. 3688–3703, 2026.
- [11] H. Jiang, Z. Wang, and Y. Liu, "Pinching-antenna system (PASS)-enhanced covert communications," *IEEE J. Sel. Areas Commun.*, vol. 44, pp. 1736–1750, 2026.
- [12] K. Wang, Z. Ding, and N. Al-Dhahir, "Pinching-antenna systems for physical layer security," *IEEE Wireless Commun. Lett.*, vol. 15, pp. 260–264, 2026.
- [13] E. Illi, M. Qaraqe, and A. Ghayeb, "Secure pinching antenna-aided ISAC," *IEEE Commun. Lett.*, vol. 30, pp. 727–731, 2026.
- [14] Z. Ding, "Pinching-antenna assisted ISAC: a CRLB perspective," *npj Wirel. Technol.*, vol. 1, no. 4, 2025.
- [15] W. Mao, Y. Lu, Y. Xu, B. Ai, O. A. Dobre, and D. Niyato, "Multi-waveguide pinching antennas for ISAC," *IEEE Trans. Wireless Commun.*, vol. 25, pp. 5846–5858, 2026.
- [16] M. Liu, Y. Xiao, J. Chen, S. Yang, X. Lei, and M. Xiao, "Integrated sensing and communication with index modulation over pinching antennas," *IEEE Commun. Lett.*, vol. 30, pp. 737–741, 2026.
- [17] C. Ouyang, Z. Wang, Y. Liu, and Z. Ding, "Rate region of ISAC for pinching-antenna systems," *IEEE Trans. Commun.*, vol. 74, pp. 5849–5866, 2026.
- [18] B. Wu, F. Fang, M. Zeng, and X. Wang, "Straggler-resilient federated learning over a hybrid conventional and pinching antenna network," *IEEE Trans. Veh. Tech.*, pp. 1–6, 2026.
- [19] S. Asaad, H. Tabassum, and P. Wang, "Pinching antennas-assisted low-latency federated learning over multi-user wireless networks," (submitted) Available on-line at arXiv:2603.08595.
- [20] Y. Lin and Z. Ding, "Tail-latency-aware federated learning with pinching antenna: Latency, participation, and placement," *IEEE Trans. Wireless Commun.*, (submitted) Available on-line at arXiv:2601.18097.
- [21] Y. Zhu, Z. Ding, and X. You, "Topological perspective of large-scale multi-cell deployment of excitable waveguide dielectrics," *IEEE Wireless Commun. Lett.*, vol. 15, pp. 151–155, 2026.
- [22] Y. Sun, Z. Ding, and G. K. Karagiannidis, "A stochastic geometric analysis on multi-cell pinching-antenna systems under blockage effect," *IEEE Wireless Commun. Lett.*, vol. 15, pp. 1085–1089, 2026.
- [23] Z. Ding, "Toward a quiet wireless world: Multi-cell pinching-antenna transmission," *IEEE Wireless Commun. Lett.*, (submitted) Available on-line at arXiv:2602.19459.
- [24] X. Chen, J. Wu, Y. Cai, H. Zhang, and T. Chen, "Energy-efficiency oriented traffic offloading in wireless networks: A brief survey and a learning approach for heterogeneous cellular networks," *IEEE J. Sel. Areas Commun.*, vol. 33, no. 4, pp. 627–640, 2015.
- [25] N. Kato, B. Mao, F. Tang, Y. Kawamoto, and J. Liu, "Ten challenges in advancing machine learning technologies toward 6G," *IEEE Wireless Commun.*, vol. 27, no. 3, pp. 96–103, 2020.
- [26] M. Vaezi, Z. Ding, and H. V. Poor, *Multiple Access Techniques for 5G Wireless Networks and Beyond*. Springer International Publishing, 2019.
- [27] C. Rosa, K. Pedersen, H. Wang, P.-H. Michaelsen, S. Barbera, E. Malkamäki, T. Henttonen, and B. Sébire, "Dual connectivity for LTE small cell evolution: functionality and performance aspects," *IEEE Commun. Mag.*, vol. 54, no. 6, pp. 137–143, 2016.
- [28] Y. Wu and L. P. Qian, "Energy-efficient NOMA-enabled traffic offloading via dual-connectivity in small-cell networks," *IEEE Commun. Lett.*, vol. 21, no. 7, pp. 1605–1608, Jul. 2017.
- [29] S. Dimatteo, P. Hui, B. Han, and V. O. Li, "Cellular traffic offloading through wifi networks," in *Proc. IEEE Eighth Int. Conf. on Mobile Ad-Hoc and Sensor Systems*, Valencia, Spain, 2011, pp. 192–201.
- [30] T. Cover and J. Thomas, *Elements of Information Theory*, 6th ed. Wiley and Sons, New York, 1991.
- [31] Z. Ding and H. V. Poor, "Analytical optimization for antenna placement in pinching-antenna systems," *IEEE Trans. Wireless Commun.*, (submitted) Available on-line at arXiv:2507.13307, 2025.
- [32] S. Boyd and L. Vandenberghe, *Convex Optimization*. Cambridge University Press, Cambridge, UK, 2003.
- [33] Z. Ding, D. Xu, R. Schober, and H. V. Poor, "Hybrid NOMA offloading in multi-user MEC networks," *IEEE Trans. Wireless Commun.*, vol. 21, no. 7, pp. 5377–5391, 2022.
- [34] "C-RAN: The road towards green RAN," China Mobile Res. Inst., Beijing, China, Oct. 2011, White Paper, ver. 2.5.
- [35] Z. Ding and H. V. Poor, "The use of spatially random base stations in cloud radio access networks," *IEEE Signal Process. Lett.*, vol. 20, no. 11, pp. 1138–1141, Nov 2013.
- [36] M. Peng, S. Yan, K. Zhang, and C. Wang, "Fog-computing-based radio access networks: issues and challenges," *IEEE Network*, vol. 30, no. 4, pp. 46–53, 2016.
- [37] H. Q. Ngo, A. Ashikhmin, H. Yang, E. G. Larsson, and T. L. Marzetta, "Cell-free massive MIMO versus small cells," *IEEE Transactions on Wireless Communications*, vol. 16, no. 3, pp. 1834–1850, 2017.